Bioorganic & Medicinal Chemistry Letters xxx (xxxx) xxxx

Contents lists available at ScienceDirect

Bioorganic & Medicinal Chemistry Letters

journal homepage: www.elsevier.com/locate/bmcl

Inhibition of hedgehog signaling by stereochemically defined *des*-triazole itraconazole analogues

Jiachen Wen, Kelly A. Teske, M. Kyle Hadden*

Department of Pharmaceutical Sciences, University of Connecticut, 69 North Eagleville Rd, Unit 3092, Storrs, CT 06029-3092, United States

ARTICLE INFO

Keywords:
Hedgehog pathway
Itraconazole
Structure-activity relationship

ABSTRACT

Dysregulation of the hedgehog (Hh) signaling pathway is associated with cancer occurrence and development in various malignancies. Previous structure-activity relationships (SAR) studies have provided potent Itraconazole (ITZ) analogues as Hh pathway antagonists. To further expand on our SAR for the ITZ scaffold, we synthesized and evaluated a series of compounds focused on replacing the triazole. Our results demonstrate that the triazole region is amenable to modification to a variety of different moieties; with a single methyl group representing the most favorable substituent. In addition, nonpolar substituents were more active than polar substituents. These SAR results provide valuable insight into the continued exploration of ITZ analogues as Hh pathway antagonists.

The Hedgehog (Hh) pathway is a signaling cascade critical for embryonic development and tissue patterning that is minimally active in healthy adults.[1] Constitutive activation of Hh signaling through a variety of different mechanisms has been implicated in developmental disorders and various types of cancers, including basal cell carcinoma (BCC), medulloblastoma (MB), and leukemia.[2–4] Inhibition of aberrant Hh pathway has been clinically verified, with several Hh pathway inhibitors approved by the U.S. FDA as single agents for the treatment of locally advanced BCC or as combination agents for acute myeloid leukemia.[5–7] All of the approved Hh antagonists and the majority of Hh inhibitors under development target Smoothened (Smo), a 7-pass transmembrane protein. Multiple mutations in Smo that reduce binding affinity and decrease overall efficacy have been reported in BCC and MB patients following relapse on vismodegib or sonidegib treatment.[3,8,9]

Itraconazole (ITZ) is a broad-spectrum triazole antifungal agent that possesses antiangiogenic and anti-Hh activity.[10–12] With respect to its antiangiogenic properties, mitochondrial protein voltage-dependent anion channel 1 (VDAC1) was identified as the molecular target, and is responsible for its antiangiogenic activity by modulating downstream PI3K/mTOR signaling.[8] ITZ is also a potent inhibitor of Hh signaling in both *in vitro* and *in vivo* of Hh-dependent cancer.[12–16] Interestingly, ITZ remains active against several clinically relevant Smo mutants in mouse embryonic fibroblasts (MEFs), suggesting the distinctness from other Smo antagonists.[17,18] Taken together, ITZ represents a promising anticancer agent, that has the ability to address the acquired resistance associated with other Smo antagonists.

Structurally, ITZ has three chiral centers and is clinically used as a mixture of four stereoisomers. A primary detriment of ITZ is that its triazole moiety can directly coordinate with the heme located in Cyp450 enzymes (including Cyp3A4), which can lead to multiple drug-drug and drug-food interactions. Our initial ITZ analogues demonstrated that removal of the triazole functionality did not affect Hh inhibition, while significantly reducing inhibition of Cyp3A4.[14] These SAR studies also demonstrated that the stereochemistry around the dioxolane region is critical for potent Hh inhibition.[14–16] Analogues with the 4*R* orientation are significantly more active than their 4*S* counterparts. By contrast, the absolute orientation at the C-2 position is less important. In addition, we demonstrated that analogues with the 2′*R* triazolone tail are generally more potent than analogous 2′*S* compounds.[14] Representative analogues **1a** and **1b** were identified as promising compounds through these previous SAR studies (Fig. 1).[14] We have synthesized a new series of ITZ analogues to explore the chemical space of the dioxolane region, including replacing the triazole moiety and probing the C-2 orientation.

The synthesis of analogues **2–6** (see Table 1 below) is shown in Scheme 1. 2′-Chloroacetophenone **9** was refluxed with imidazole/phthalimide to afford the appropriate *N*-substituted acetophenone. Ketones **9–11** were refluxed overnight with (*S*)-3-tosyl-1,2-propanediol utilizing a Dean–Stark apparatus. Both 2*R* and 2*S* dioxolanes were formed simultaneously, and were subsequently separated through preparative TLC to give (2*R*,4*R*)- and (2*S*,4*R*)-dioxolanes in a 1:1 ratio. An alternative synthetic route was utilized when a strong electron withdrawing group (EWG) located at the ketone α-position. Ketone **13**

* Corresponding author.
E-mail address: kyle.hadden@uconn.edu (M. Kyle Hadden).

https://doi.org/10.1016/j.bmcl.2019.126794
Received 23 September 2019; Received in revised form 28 October 2019; Accepted 30 October 2019

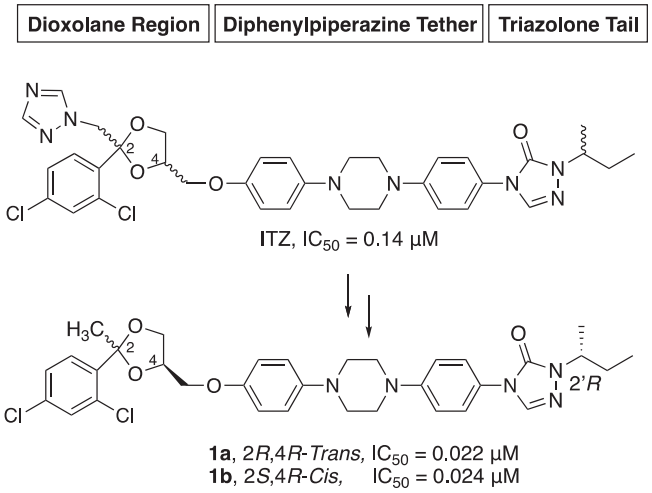

Fig. 1. Initial SAR for the ITZ scaffold.

was condensed with (*R*)-3-chloro-1,2-propanediol under alkaline conditions to give diastereomers with a free hydroxyl, which was subsequently tosylated to give **18a** and **18b** in 1:1 ratio. Finally, dioxolanes **14–18** were coupled with phenol **19**, synthesized as earlier report,[14] to afford diastereomers **2–6**.

To determine the absolute stereochemistry of each diastereomer at the dioxolane C-2 position, we carefully analyzed the ^{1}H NMR spectra of each analogue. Through this analysis we identified a clear difference in the chemical shift based on the orientation adopted by the phenyl ring. Taking **14a** and **14b** as an example (Fig. 2), when the phenyl ring is in close proximity to the C-4 proton (below the plane), the chemical shift of the C-4 proton is lower (δ = 4.37) because of the "shielding effect" provided by the phenyl moiety.[19] By contrast, when the phenyl ring is located away from the C-4 proton and is not shielded, the chemical shift is located further downfield (δ = 4.68). The same trends were universally observed in all the dioxolane analogues synthesized here, and they closely match those we have previous synthesized, which were unambiguously characterized by X-ray crystallization.[14]

The synthesis of analogues **7** and **8** (Table 1) is summarized in Scheme 2. 2,4-Dichloroiodobenzene (**20**) was condensed with diethyl oxalate through Grignard procedures to give α-oxo-benzeneacetaldehyde **21** in good yield. As mentioned previously, when an EWG is appended to the ketone α-position, alkaline rather than acidic conditions should be applied to construct the dioxolane core. Interestingly, instead of yielding the dioxolane diastereomers, endocyclic compound **22** was identified as the only product. Upon further consideration, this result was not surprising since the intramolecular ester exchange is readily available under alkaline conditions. Only the 2*S*,4*S*-*cis* bicyclic dioxolane was observed due to the proper stereo position. Intermediate **22** was gently heated with ammonium hydroxide to give primary amide **23** in quantitative yield through aminolysis. After tosylation, **24** was readily coupled with phenol **19** to give analogue **7**. Amide **7**, which was further reduced to primary amine **8** with lithium aluminum hydride.

As noted above, our previous SAR studies for the ITZ scaffold demonstrated that the triazole is not required for potent Hh inhibition.[14] In order to continue our SAR exploration of this region, we sought to synthesize and evaluate analogues that contain the general stereochemically defined ITZ scaffold represented by **1a** and **1b**. As shown in Table 1, we evaluated these analogues for their ability to decrease Gli1 mRNA expression in the Hh-dependent murine BCC cell line ASZ001.[20–22] Replacing the triazole of ITZ with an imidazole, (**2a** and **2b**) resulted in analogues with activity equivalent to each other and slightly improved (IC_{50} = 0.11 μM for both) compared to ITZ.

Table 1
Anti-Hh activity for ITZ and its analogues.[a]

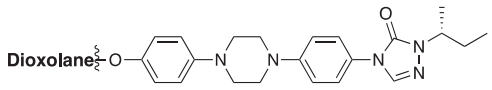

Cmpd.	Dioxolane Region	Stereochemistry	IC_{50} in ASZ001, μM
ITZ	/	/	0.14 ± 0.02
1a*	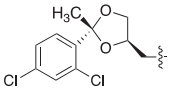	2*R*,4*R*-*Trans*	0.022 ± 0.01
1b*	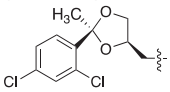	2*S*,4*R*-*Cis*	0.024 ± 0.02
2a	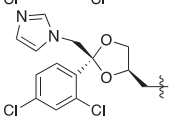	2*S*,4*R*-*Cis*	0.11 ± 0.02
2b	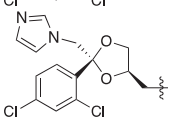	2*R*,4*R*-*Trans*	0.11 ± 0.04
3a	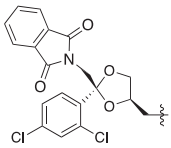	2*S*,4*R*-*Cis*	0.82 ± 0.09
3b	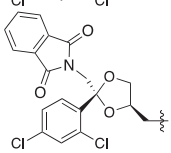	2*R*,4*R*-*Trans*	1.07 ± 0.13
4a	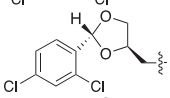	2*R*,4*R*-*Trans*	0.31 ± 0.14
4b	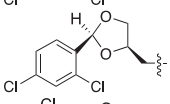	2*S*,4*R*-*Cis*	0.30 ± 0.11
5a	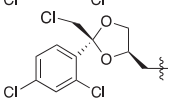	2*S*,4*R*-*Cis*	0.025 ± 0.012
5b	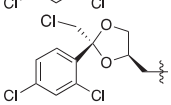	2*R*,4*R*-*Trans*	0.020 ± 0.014
6a	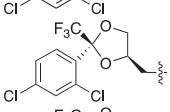	2*S*,4*R*-*Cis*	0.067 ± 0.013
6b	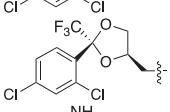	2*R*,4*R*-*Trans*	0.069 ± 0.008
7	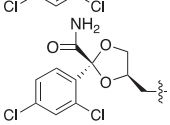	2*S*,4*R*-*Cis*	0.94 ± 0.08
8	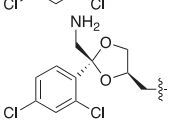	2*S*,4*R*-*Cis*	0.55 ± 0.12

[a] IC_{50} values represent the Mean ± SEM of at least two separate experiments performed in triplicate. *Adapted from ref. [14].

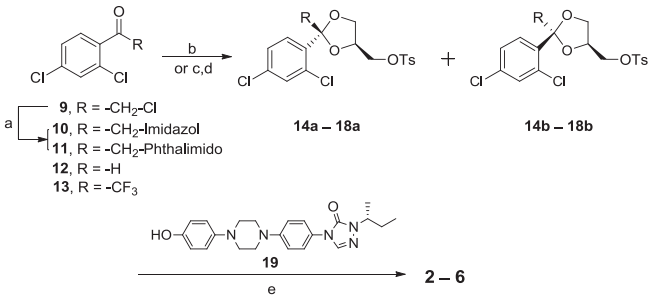

Scheme 1. Reagents and conditions. (a) Imidazole/Phthalimide, K_2CO_3, CH_3CN, reflux, 4 h, 96–98%; (b) TsOH (cat.), toluene, reflux/RT, overnight, 23–88% (**a**:**b** in 1:1 ratio); (c) (*R*)-3-Chloro-1,2-propanediol, K_2CO_3, DMF, RT, overnight, 91%; (d) TsCl, pyridine, CH_2Cl_2, RT, overnight, 93% (**a**:**b** in 1:1 ratio); (e) Cs_2CO_3, DMF, 80 °C/RT, 4 h, 32–87%.

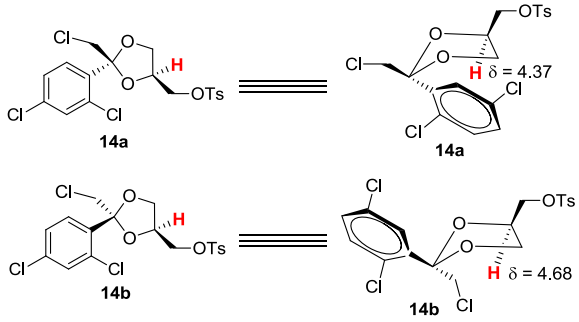

Fig. 2. Elucidating the absolute stereochemistry by ^{1}H NMR.

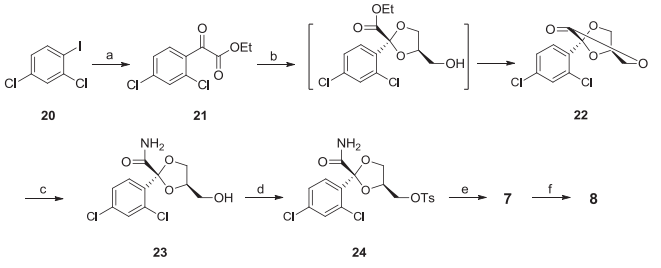

Scheme 2. Reagents and conditions. (a) Diethyl oxalate, Mg, I_2, Et_2O, RT, 4 h, 89%; (b) (*R*)-3-Chloro-1,2-propanediol, Cs_2CO_3, DMF, RT, overnight, 95%; (c) Ammonium hydroxide, 25% in water, 50 °C, 4 h, quant.; (d) TsCl, pyridine, CH_2Cl_2, RT, overnight, 72%; (e) **19**, Cs_2CO_3, DMF, 80 °C, 4 h, 71%; (f) $LiAlH_4$, THF, 0 °C, 30 min, 28%.

Increasing the substituent size to a fused-cycle phthalimide (**3a** and **3b**) lead to a sharp decrease in activity (IC_{50} values of approximately 1.0 μM); while completely removing the triazole group (**4a** and **4b**, R = H) lead to a moderate drop in activity (IC_{50} values of approximately 0.3 μM).

Taking these initial results into consideration, we thought that a single methyl group might represent the optimal size substituent at the C-2 dioxolane position to fit into the sub-pocket. Analogues with bulkier (ITZ, **2**, and **3**) or no substituent (**4**) were significantly less active than the analogues containing methyl groups (**1a** and **1b**). With this in mind, we further designed and synthesized ITZ analogues bearing methyl bioisosteres. Not surprisingly, when a chloromethyl replaces the methyl group, these analogues (**5a** and **5b**) showed potent activity against the Hh pathway (with IC_{50} values = 0.025 and 0.02 μM, respectively). Introducing a trifluoromethyl group (**6a** and **6b**) resulted in a slight decrease in activity compared to **1a** and **1b**. These results provide further evidence that moieties maintaining the approximate size of a methyl group are optimal for activity of our scaffold.

In parallel to the analogues described above, we sought to replace the triazole with an amine, which led to the synthesis of analogue **8**. The purpose of preparing this analogue was two-fold. First, our previously prepared ITZ analogues demonstrate poor solubility and we hypothesized that addition of the primary amine could enhance this essential pharmacokinetic property. Second, we thought that the amine would be a promising chemical handle to attach additional functionality to the scaffold. Interestingly, analogue **8** was significantly less active than the other analogues with methyl mimics in the triazole position (IC_{50} = 0.55 μM). Amide intermediate **7** was less active (IC_{50} = 0.94 μM), suggesting a polar group in the dioxolane 2-position is unfavorable for potent anti-Hh activity. Based on our initial results showing increased bulk at this position is detrimental to anti-Hh activity, we did not make additional analogues with triazole mimics linked through the amine.

We utilized topological polar surface area (TPSA) in an attempt to quantify the influence of polarity in the triazole region on anti-Hh activity. Based on the calculation, a correlation between TPSA and Hh inhibition is summarized in Fig. S1. Our results demonstrate the TPSA is preferred to be approximately 70 Å^2, as represented by analogues **1** and **5**. Analogues with TPSA above 70.1 Å^2 (up to 113.2 Å^2) were less active suggesting the hydrophobic nature of the binding sub-pocket for this region. In addition, a TPSA value below 90 Å^2 also correlates with enhanced cell permeability.[23]

In conclusion, a series of stereochemically defined ITZ analogues focused on triazole modifications was synthesized and evaluated to continue our SAR studies of ITZ analogue inhibition of Hh signaling. These modifications ranged in size from proton to phthalimide. Based on our results, a single methyl group represents the most favorable substituent on dioxolane C-2 position. In addition, there is no significant difference in Hh inhibition between 2*R,4R* and 2*S,4R* diastereomers, suggesting the stereochemistry on dioxolane C-2 position, is less important for potent Hh inhibition. Finally, a nonpolar substituent is better than a polar substituent, suggesting the hydrophobic nature of the binding pocket. This study would be useful for the understanding of the chemical space of the dioxolane region, as well as developing next generation ITZ analogues as Hh-pathway antagonists.

Declaration of Competing Interest

The authors declare that they have no known competing financial interests or personal relationships that could have appeared to influence the work reported in this paper.

Acknowledgments

The authors gratefully acknowledge support of this work by the National Institutes of Health/National Cancer Institute (CA190617). ASZ001 cells were provided by Dr. Ervin Epstein (Children's Hospital Oakland Research Institute).

Appendix A. Supplementary data

Supplementary data to this article can be found online at https://doi.org/10.1016/j.bmcl.2019.126794.

References

1. Banerjee U, Hadden MK. *Expert Opin Drug Discov.* 2014;9:751.
2. Yang L, Xie G, Fan Q, Xie J. *Oncogene.* 2010;29:469.
3. Dagklis A, Pauwels D, Lahortiga I, et al. *Haematologica.* 2015;100:e102.
4. Burns MA, Liao ZW, Yamagata N, et al. *Leukemia.* 2018;32:2126.
5. Ghirga F, Mori M, Infante P. *Bioorg Med Chem Lett.* 2018;28:3131.
6. Savona MR, Pollyea DA, Stock W, et al. *Clin Cancer Res.* 2018;24:2294.
7. Peer E, Tesanovic S, Aberger F. *Cancers.* 2019;11:538.
8. Pricl S, Cortelazzi B, Dal Col V, et al. *Mol Oncol.* 2015;9:389.
9. Wahid M, Jawed A, Mandal RK, et al. *Crit Rev Oncol Hemat.* 2016;98:235.
10. Head SA, Shi W, Zhao L, et al. *Proc Natl Acad Sci U S A.* 2015;112:e7276.

11. Tsubamoto H, Ueda T, Inoue K, et al. *Oncol Lett.* 2017;14:1240.
12. Kim J, Tang JY, Gong R, et al. *Cancer Cell.* 2010;17:388.
13. Shi W, Nacev BA, Aftab BT, et al. *J Med Chem.* 2011;54:7363.
14. Pace JR, DeBerardinis AM, Sail V, et al. *J Med Chem.* 2016;59:3635.
15. Pace JR, Kelly AT, Lianne QC, et al. *J Med Chem.* 2019;62:3873.
16. Wen J, Chennamadhavuni D, Morel SR, et al. *ACS Med Chem Lett.* 2019;10:1290.
17. Kim J, Aftab BT, Tang JY, et al. *Cancer Cell.* 2013;23:23.
18. Tao H, Jin Q, Koo DI, et al. *Chem Biol.* 2011;18:432.
19. Matsugi M, Itoh K, Nojima M, et al. *Tetrahedron Lett.* 2001;42:6903.
20. DeBerardinis AM, Madden DJ, Banerjee U, et al. *J Med Chem.* 2014;57:3724.
21. Wen J, Hadden MK. *ChemMedChem.* 2018;13:748.
22. Teske KA, Dash RC, Morel SR, et al. *Euro J Med Chem.* 2019;163:320.
23. Hitchcock SA, Pennington LD. *J Med Chem.* 2006;49:7559.